

Bandwidth Enhancement of Slot Antenna Using Fractal Shaped Isosceles for UWB Applications

Djelloul Aissaoui^{1,2}, Abdelhalim Chaabane³, Nouredine Boukli-Hacene², and Tayeb A. Denidni⁴

¹Faculté des sciences Technologiques
Université Ziane-Achour de Djelfa, 17000, Algeria
djelloul.aissaoui@univ-djelfa.dz

²Laboratoire De Télécommunications
Université De Tlemcen, BP 230, Pole Chetouane, Tlemcen 13000, Algeria
abdelhafid.bouacha@gmail.com

³Laboratoire des Télécommunications, Département d'Electronique et Télécommunications
Faculté des Sciences et de la Technologie, Université 8 Mai 1945 Guelma, BP 401, Guelma 24000, Algeria
abdelhalim.chaabane@univ-guelma.dz

⁴Institut National de la Recherche Scientifique
Centre EMT, 800 Rue De La Gauchetière West, Suite 6900, Montreal, Quebec, H5A-1K6, Canada
denidni@emt.inrs.ca

Abstract – In this paper, a coplanar waveguide (CPW) fed slot antenna using fractal shaped isosceles trapezoidal corrugations is designed and presented for Ultra-Wideband (UWB) applications. The proposed antenna is formed by a regular hexagonal patch fed through a CPW feed line and radiates amidst a notched wide hexagonal slot. The edge of the wide slot is shaped by a fractal structure that is formed by five trapezoidal notches. The antenna is printed on RO4350B substrate having a compact size of $0.305\lambda_0 \times 0.313\lambda_0 \times 0.012\lambda_0$ at 2.35 GHz. Good agreement is registered between the experimental results of the fabricated prototype and the calculated ones. By using an Agilent 8722ES vector network analyzer, the fabricated prototype confirms that the antenna has an excellent matching impedance over the bandwidth 2.35-10.65 GHz (127%) which covers the entire UWB band. Furthermore, good radiation performances are measured in an anechoic chamber. Consistent radiation patterns with a reasonable peak gain are measured over the entire working bandwidth. Therefore, the designed structure may be worthy considered for different wireless communications systems.

Index Terms – coplanar waveguide (CPW), fractal antenna, isosceles trapezoidal corrugations, slot antenna, ultra-wideband (UWB) antenna.

I. INTRODUCTION

Over the last few years, the appliance of the Ultra-wideband (UWB) technologies for modern wireless communication systems has received much appreciation owing to their promote features over a wide transmission capacity, such as low power level consuming, low signal disturbances, opportunity of low-cost transceivers, simplicity, and higher data transmission rate [1–3]. UWB systems have attracted enormous preoccupation due to the large bandwidth of 7.5 GHz extending from 3.1 to 10.6 GHz, which was attributed by the Federal Communications Commission in February 2002 [4]. In today's world, UWB technology has been applied for several applications, such as radar detection, satellite communications, and vehicular communications systems [5]. Recently, enormous attempts have been concentrated on the expansion of UWB microwave components to become more compact and to improve their performances [6]. Typically, printed monopole planar antennas offer the main requirements and considered as excellent devices for UWB applications; dues to the characteristics that are proposed, such as low cost, low profile, compact sizes, possibility of incorporation with other RF devices, larger bandwidth, and consistent radiation patterns with acceptable gains over the considered bandwidths. For these reasons, the development of UWB antennas has spurred academic and industrial research. In recent few

years, several UWB planar antennas with miscellaneous configurations have been designed. In this respect, various techniques have been used to improve the main requested bandwidth such as the use of large etched slot in the ground plane as in [7]. Another method is to use fractal structures that are also able to diminish the attributed size and to enhance the antenna adaptation as in [8]. Unfortunately, most of the existing antennas in the literature don't cover the entire licensed UWB bandwidth and/or have complex and large configurations. In [9], an octagonal ring shaped antenna was proposed for UWB application. However, the main disadvantage of this antenna is that it doesn't cover the entire licensed UWB range. A bi-directional tapered slot antenna that has a large size of $55 \times 48 \times 1.5 \text{ mm}^3$ has been proposed in [10]. A probe-fed hexagonal UWB antenna with AMC reflector having a complex structure and a bulky size of $100 \times 100 \times 15 \text{ mm}^3$ has been proposed in [11]. A narrow-band Fabry Perot cavity UWB antenna that has a complex structure and a large size of $169 \times 169 \times 38.46 \text{ mm}^3$ has been introduced in [12]. In [13], a narrow band antipodal UWB Vivaldi antenna that has a complex structure and a bulky size of $100 \times 104 \times 1.5 \text{ mm}^3$ has been proposed. A closed loop resonator based compact UWB antenna that has a complex structure and a large size of $100 \times 100 \times 16 \text{ mm}^3$ has been proposed in [14]. A complex geometry that covers only the frequency range of 1.31 – 6.81 GHz has been presented in [15].

II. ANTENNA CONFIGURATION AND DESIGN

The geometrical configuration of the proposed wide hexagonal slot fractal antenna is presented in Fig. 1. It is designed using RO4320B substrate having a relative permittivity $\epsilon_r = 3.66$, a thickness of 1.524 mm and a loss tangent of 0.004. The proposed CPW-fed UWB slot antenna is basically composed of a wide-hexagonal-slot antenna and a parasitic hexagonal patch fed by a CPW. Thus, there are two radiating elements: the wide-hexagonal-slot and the hexagonal patch which acts as a tuning stub. Moreover, five trapezoidal slots are inserted symmetrically on the perimeter of the wide-hexagonal-slot antenna to improve the impedance characteristics. The hexagonal patch antenna has been designed by relating the areas of a circular patch with the one of the hexagonal patch structure. As given in [16], the side length B of a hexagonal patch can be calculated using the equation

$$B \approx 1.1 r_e, \quad (1)$$

where r_e is the equivalent radius of a comparable circular patch given by the formula

$$r_e = \sqrt{r^2 - \frac{2hr}{\pi\epsilon_r} \left(\ln \frac{\pi r}{2h} + 1.7726 \right)}, \quad (2)$$

where ϵ is the dielectric constant of the substrate, c is the speed of light in free space, h is the thickness of the substrate, and r is the radius of a comparable circular patch. The resonant frequency f_r of the hexagonal patch can be calculated using the formula (3).

$$f_r \approx \frac{Y_{mn}c}{2\pi r_e \sqrt{\epsilon_r}}, \quad (3)$$

where Y_{mn} is the m^{th} zero of the derivative of the Bessel function of order n . The values of Y_{mn} are given in Table 1.

Table 1: Values of Y_{mn}

Modes	Y_{mn}
TM01	0
TM11	1.841
TM21	3.054
TM02	3.832
TM31	4.201
TM41	5.317
TM51	6.415

The edge of the proposed wide slot is constituted by a fractal structure that is formed by notching a succession of five regular isosceles trapezoidal from the middle of the ribs constituting the hexagonal slot that having a length of $A = 16.2 \text{ mm}$. The isosceles trapezoidal notches have three identical ribs of length $h_1 = 3.2 \text{ mm}$ and one lengthy rib of length $h_2 = 6.4 \text{ mm}$.

The radiating element is lodged inside a ground plane having the same outer dimensions of the substrate of $0.305\lambda_0 \times 0.313\lambda_0$ at 2.35 GHz. The patch consists of a regular hexagon with a length of $B = 10.5 \text{ mm}$ and is fed by a CPW with an input impedance of value 50Ω . The strip width W_f and the gap g between the feed line and the ground plane have of values 2.9 mm and

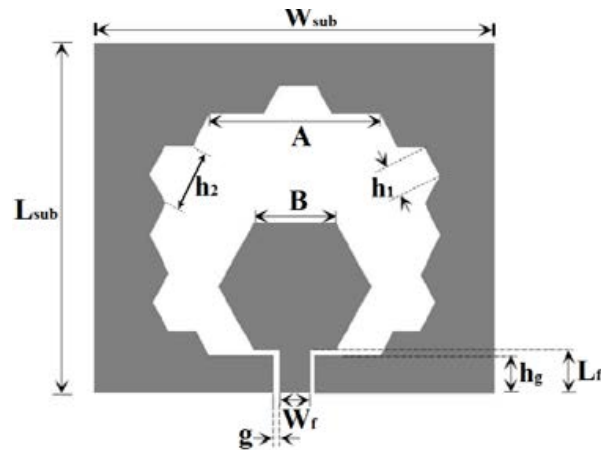


Fig. 1. Geometrical configuration of the proposed UWB slot antenna.

0.275 mm, respectively. As illustrated in Fig. 1, the designed antenna has a compact size of $0.305\lambda_0 \times 0.313\lambda_0 \times 0.012\lambda_0$ at 2.35 GHz. The detailed dimensions of the proposed UWB fractal antenna are listed in Table 1.

III. RESULTS AND PARAMETRIC STUDY

The electromagnetic solver, CST Microwave Studio [17], was used to numerically calculate and optimize the proposed fractal antenna. The reflection coefficient $|S_{11}|$ of the simulated antenna, with the optimized parameters listed in Table 1, is depicted in Fig. 2. As a consequence of applying isosceles trapezoidal fractal elements on the proposed antenna the impedance bandwidth is enlarged by a 4.79 GHz; the high-frequency side is shifted up from 8.35 GHz to 12.75 GHz and the low-frequency side of the working bandwidth is also shifted down from 2.66 GHz to 2.27 GHz. Thereby, a 60.8% fractional bandwidth expansion is achieved (from 77.7% to 138.5%). Therefore, a UWB ranging from 2.27 to 12.75 GHz is exhibited which covers the entire UWB spectrum from 3.1 to 10.6 GHz. to show the effect of

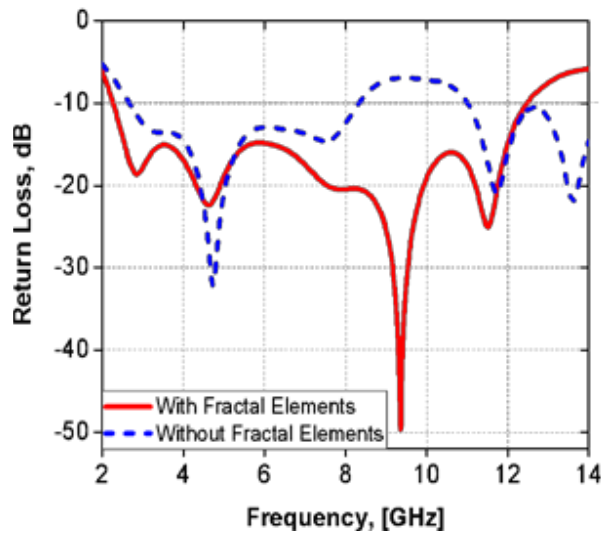


Fig. 2. Simulated return loss of the two antennas: for referenced antenna (dashed line); for the proposed UWB slot antenna (solid line).

Table 2: Optimized dimensions of the proposed slot antenna in term of wavelength at 2.35 GHz

Parameters	Dimensions [m]	Parameters	Dimensions [m]
A	$0.1269\lambda_0$	L_{sub}	$0.3055\lambda_0$
B	$0.0823\lambda_0$	W_{sub}	$0.3133\lambda_0$
h_1	$0.0251\lambda_0$	W_f	$0.0227\lambda_0$
h_2	$0.0501\lambda_0$	L_f	$0.0760\lambda_0$
h_g	$0.0204\lambda_0$	g	$0.0021\lambda_0$

the antenna parameters on the bandwidth performance, a parametric study was carried out by changing one of the parameters while keeping all other parameters fixed as listed in Table 2. The first parametric study is on the length h_1 of the trapezoidal fractal notch elements. The influence of this parameter on the impedance bandwidth and the adaptation of the simulated antenna for different values 0.5, 1.5, 3.2, 4.5, and 5.5 mm are plotted in Fig. 3 (a). It can be seen that as the length h_1 augments from 0.5 to 3.2 mm the impedance bandwidth increases greatly by 36.52% (from 102.07% to 138.62%). However, the bandwidth decreases when the length h_1 exceeds 3.2 mm. Therewithal, the optimal length of the trapezoidal corrugations is found to be at $h_1=3.2$ mm. In addition, the lower frequencies of the bandwidth change slightly by increasing the length h_1 of the trapezoidal notches, while at the middle and the high frequencies, the augmentation of this parameter combines the resonances of the bandwidth that leads to improving the upper frequency of the bandwidth from 8.3 to 12.4 GHz

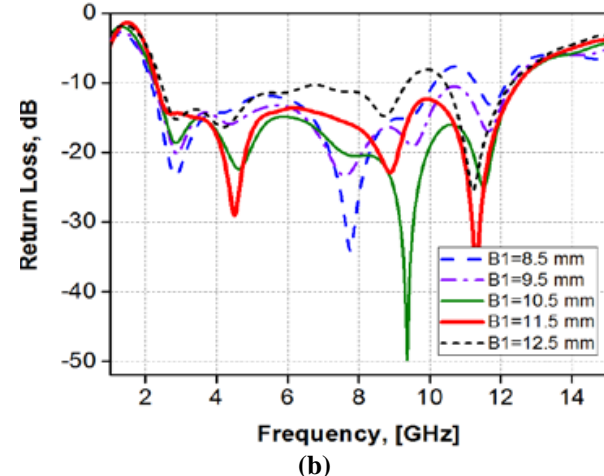
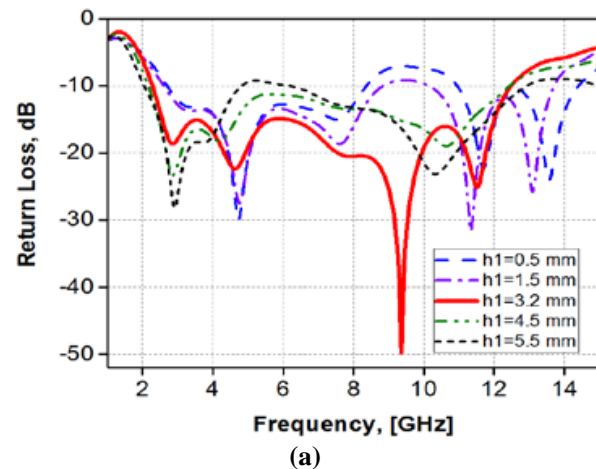


Fig. 3. Continued.

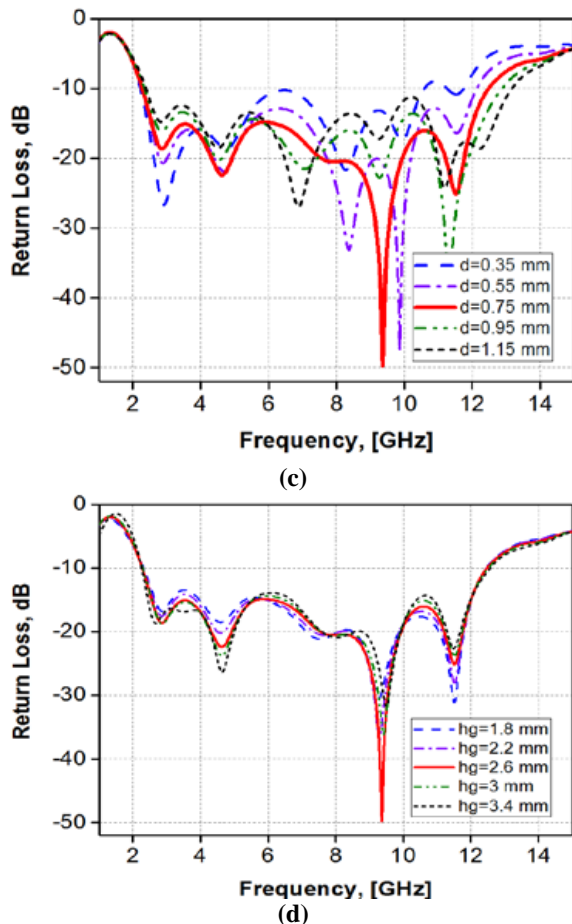


Fig. 3. Effect of different parameters on the reflection coefficient of the proposed antenna: (a) effect of the trapezoidal notch length; (b) effect of the parasitic patch length; (c) effect of the gap between the parasitic patch and the ground plane; (d) effect of the ground plane length.

and, consequently, the UWB characteristic of the proposed antenna is achieved. Therefore, the parameter h_1 represents a major impact on the impedance-matching performance of the proposed antenna. The impact of adjusting the patch side length B on the bandwidth performance is also studied. The antenna was calculated for different values of parameter B commencing from 7.5 to 11.5 mm with an increment of 1 mm, the obtained results are presented in Fig. 3 (b). As can be observed, the impact of patch length B on the impedance bandwidth and the adaptation performances is clearly visible. It is shown that the antenna bandwidth becomes wider by 9% (from 129.62% to 138.62%) when increasing the side length B from 7.5 to 10.5 mm. However, the bandwidth does not augment any further when the side length exceeds 10.5 mm. It can be noticed that as the patch augments in length a better adaptation performance is achieved over the working bandwidth. As illustrated in Fig. 3 (b), when

B_1 exceeds 9.5 mm, the matching characteristics of the proposed antenna are enhanced at 10.7 GHz. When the length B_1 exceeds 10.5 mm, the $|S_{11}|$ becomes narrower because of the growth of the capacitive coupling between the radiating element and the ground plane. Thus, the patch leads to augmenting greatly the upper frequency of the operating bandwidth. Thereby, the optimum value of the parameter B_1 is taken at 10.5 mm. The mutual coupling between the feed and the patch has an important impact on the antenna adaptation performance. For this reason, the impact of the gap d separating the patch and the ground plane is furthermore studied. Figure 3 (c) depicts the $|S_{11}|$ for various values of gap d varying between 0.35 and 1.15 mm with an increment of 0.2 mm. As it is shown, this gap d augments the upper side of the bandwidth augments, whereas, the lower side is nearly invariable. Therefore, the adaptation improves and the total impedance bandwidth augments. The optimum distance separating the patch and the ground plane is obtained at 0.75 mm. When the gap d exceeds 0.75 mm, the $|S_{11}|$ becomes narrower because the antenna impedance matching is going bad.

Figure 3 (d) presents the impact of the ground plane length h_g on the $|S_{11}|$. Its influence was studied for different lengths of the ground plane ranging from 1.8 to 3.4 mm with an increment of 0.4 mm. It can be seen that as the length h_g augments, the lower side of the impedance bandwidth as well as the upper side of the bandwidth changes slightly. Therefore, it is clearly observed that the length h_g has not a considerable impact on the antenna bandwidth. The optimum ground plane length for the proposed antenna was optimized at 2.6 mm.

IV. MEASURED RESULTS AND DISCUSSION

To give credence to the calculated results, a prototype of the proposed UWB slot antenna with the optimized geometrical dimensions were constructed and measured. Figure 4 presents a photograph of the realized prototype. The reflection coefficient $|S_{11}|$ of the fabricated antenna is then measured using an Agilent 8722ES vector network analyzer. Figure 5 shows the measured reflection coefficient against their simulated results. It indicates that the fabricated antenna exhibits a measured impedance bandwidth as large as 8.32 GHz and covers the band ranging from 2.35 GHz to 10.67 GHz, relatively about 127%, which is suitable for UWB applications.

The comparison between simulated and measured results of the coefficient reflection indicates that there is a slight difference. At lower frequencies, an excellent concordance is observed between the calculated and measured results. Besides, there is a little disagreement at high frequencies which is mainly due to the fabrication tolerance and connector soldering.

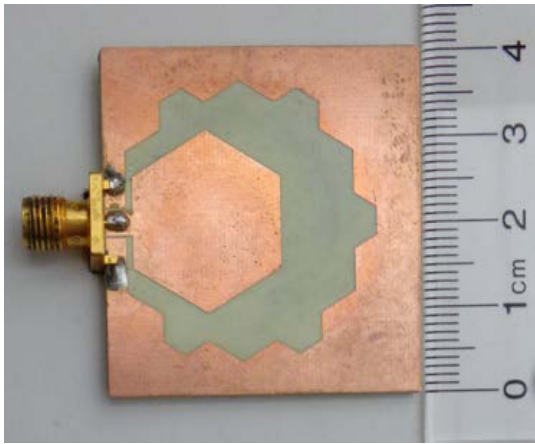


Fig. 4. Photograph of the proposed CPW-fed UWB slot antenna.

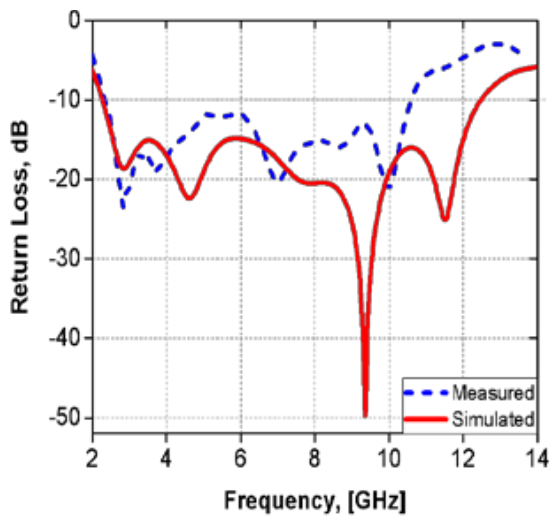


Fig. 5. Simulated and measured return loss S_{11} [dB] against frequency.

Furthermore, the H- and E- plane patterns of the fabricated antenna were measured in an anechoic chamber and compared with the predicted ones. Figure 6 shows the both measured and simulated 2-D far-field radiation patterns of the fabricated antenna in two principal planes, the E and H-planes for three respective frequencies 3, 5, and 9.5 GHz. Excellent agreements are achieved between the measured results and the calculated ones. In addition, the quasi-omnidirectional patterns can be observed in the H-plane at all frequencies, while in the E-plane, a bidirectional radiation pattern is achieved at the frequencies 3 and 5 GHz. At high frequencies around 9.5 GHz, the measured radiation pattern in the E-plane is no longer bidirectional. The small deformation at higher frequencies is probably due to the excitation of higher-order modes [18–19]. Figure 7 depicts the measured and

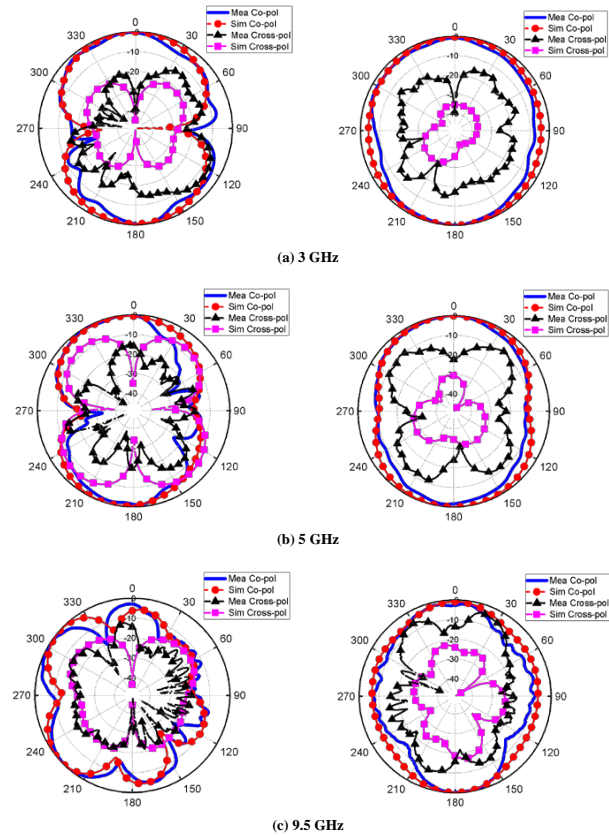


Fig. 6. Measured and simulated normalized radiation patterns of the proposed UWB slot antenna in E-plane (left) and H-plane (right) at three frequencies: (a) 3 GHz, (b) 5 GHz, and (c) 9.5 GHz.

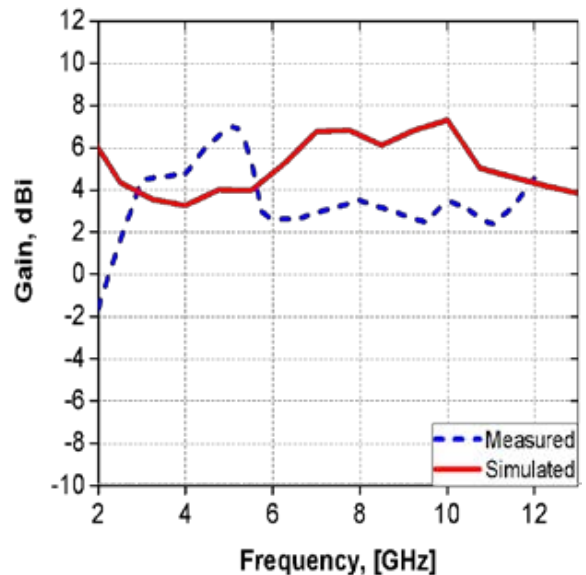


Fig. 7. Gain of the proposed UWB slot antenna versus frequency.

Table 3: Comparison of the fabricated antenna with other recently published antennas

Ref. No.	Antenna structure	Ground plane (GP)	Substrate/ permittivity	Electrical size	Bandwidth (GHz)	Bandwidth (%)	Peak Gain (dBi)	Ease of fabrication
[24]	Microstrip line-fed monopole antenna	Partial GP	FR4 $\epsilon_r=4.6$	$0.338\lambda_0$ $\times 0.347\lambda_0$ $\times 0.014\lambda_0$	2.6-12.3	130.2	5.52	Easy
[25]	CPW-fed U-shaped monopole antenna	Partial GP	FR4 $\epsilon_r=4.4$	$0.402\lambda_0$ $\times 0.435\lambda_0$ $\times 0.0201\lambda_0$	4.02-10.7	90.76	3.54	Easy
[26]	L-shaped feed line aperture antenna	Slotted GP	FR4 $\epsilon_r=4.4$	$0.568\lambda_0$ $\times 0.568\lambda_0$ $\times 0.0116\lambda_0$	2.9-8	93.5	4.9	Easy
[27]	CPW-fed printed monopole antenna	Partial GP	FR4 $\epsilon_r=4.4$	$0.358\lambda_0$ $\times 0.358\lambda_0$ $\times 0.0057\lambda_0$	2.15- 6.97	105.70	5	Easy
[28]	Metasurface-based microstrip-fed planar antenna	Partial GP	FR4 $\epsilon_r=4.4$	$0.34\lambda_0$ $\times 0.34\lambda_0$ $\times 0.05\lambda_0$	3.1-10.6	109.49	6.8	Hard
[29]	Coaxial probe-fed microstrip patch with metamaterial-inspired reactive impedance surface	Full GP	RO4003 $\epsilon_r=3.38$	$0.58\lambda_0$ $\times 0.58\lambda_0$ $\times 0.1\lambda_0$	4.64-7.3	44.5	7.2	Hard
[30]	CPW-fed cauliflower shaped antenna	Partial GP	RO-4350B $\epsilon_r=3.48$	$0.368\lambda_0$ $\times 0.417\lambda_0$ $\times 0.015\lambda_0$	3.05-10.96	113	5.68	Hard
[31]	Microstrip line-fed question mark shaped antenna	Partial GP	FR4 $\epsilon_r=4.4$	$0.347\lambda_0$ $\times 0.393\lambda_0$ $\times 0.017\lambda_0$	3.47-12.11	110.91	6	Easy
This work	CPW-fed slot antenna with fractal shaped isosceles trapezoidal	Slotted GP	RO-4350B $\epsilon_r=3.66$	$0.305\lambda_0$ $\times 0.313\lambda_0$ $\times 0.012\lambda_0$	2.35-10.65	127	7.02	Easy

simulated peak gain of the fabricated prototype. Acceptable values are achieved in the whole UWB range with a maximum gain of 7.02 dBi attained at about the frequency of 5.15 GHz. The discrepancy between the simulated and measured gains may be due to many reflections into the electromagnetic waves between the tested antenna and reference antenna (double ridged horn antenna AH-118 operating between 1 and 18 GHz). The reflections may come from the room floor and ceiling, chamber scattering, and track inside the anechoic cham-

ber. Figure 8 shows that the designed CPW-UWB slot antenna reveals acceptable values of efficiency within the operating band which are nearly over 80% that are superior to the ones achieved in [20–21]. The simulated group delay along the working bandwidth is plotted in Fig. 9 for a distance of 30cm between the front faces of two similar CPW-fed UWB slot antennas. A feeble variation below 1ns is obtained which is nearly comparable to the results presented in [22–23]. To demonstrate the usefulness of the fabricated model, the main parameters of the

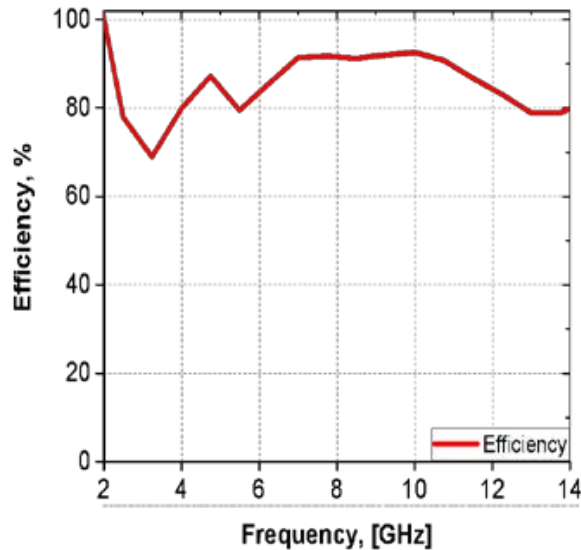


Fig. 8. Efficiency of the proposed UWB slot antenna versus frequency.

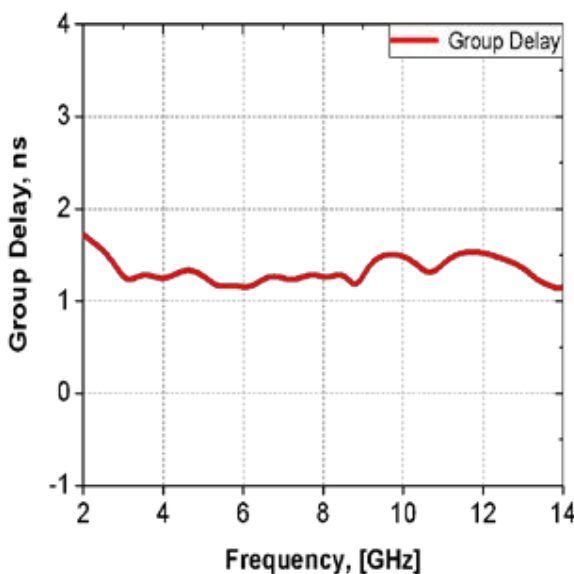


Fig. 9. Group delay of the proposed UWB slot antenna versus frequency.

proposed antenna are compared with the ones of some existing antennas in Table 3. It can be deduced that the parameters of the fabricated model are better or comparable to those of other existing antennas.

V. CONCLUSION

A compact printed CPW-fed slot antenna using fractal-shaped isosceles trapezoidal corrugations for UWB applications has been designed and measured in this work. The implementation of the isosceles trapezoidal fractal structure along the edge

of the hexagonal slot has improved the working bandwidth. Experiments have been implemented to prove the antenna performances confirming that the fabricated antenna offers a large impedance bandwidth of about 127%, extending from 2.35 GHz to 10.67 GHz; which covers the entire UWB. Moreover, stable radiation patterns measured with an acceptable peak gain are measured over the whole working bandwidth. Thus, it can be concluded that the proposed design can be an advantageous candidate for many wireless communication systems.

ACKNOWLEDGMENT

This work was supported by the Directorate-General for Scientific Research and Technological Development (DG-RSDT) of Algeria.

REFERENCES

- [1] D. Aissaoui, A. Chaabane, and A. Bouacha, "Compact super UWB elliptical antenna with corrugations for wireless communication systems," *IEEE IRASET 1st Int. Conf. Innov. Res. App. Sci. Eng. Technol.*, Meknes, MA, pp. 1-4, Apr. 2020.
- [2] A. Chaabane and A. Babouri, "Dual band notched uwb MIMO antenna for surfaces penetrating application," *Adv. Electromagn.*, vol. 8, no. 3, pp. 6-15, 2019.
- [3] A. Chaabane, O. Mahri, D. Aissaoui, and N. Guebgoub, "Multiband stepped antenna for wireless communication applications," *Inf. MIDEM.*, vol. 50, no. 4, pp. 275-284, 2020.
- [4] E. Wang, W. Wang, X. Tan, Y. Wu, J. Gao, and Y. Liu, "A UWB MIMO slot antenna using defected ground structures for high isolation," *Int. J. RF Microw. Comput.-Aided Eng.*, vol. 30, no. 5, pp. 1-10, 2020.
- [5] B. Hammache, A. Messai, I. Messaoudene, and T. A. Denidni, "Compact ultrawideband slot antenna with three notched-band characteristics," *Int. J. RF Microw. Comput.-Aided Eng.*, vol. 30, no. 5, pp. 1-10, 2020.
- [6] A. F. Daw, M. A. Abdalla, and H. El-Henawy, "Wideband slow phase loaded inductor-composite right/left-handed transmission line for compact UWB power divider," *Microw. Opt. Technol. Lett.*, vol. 62, no. 6, pp. 1-5, 2020.
- [7] R. Azim, M. T. Islam, and N. Misran, "Compact tapered shape slot antenna for UWB applications," *IEEE Antennas Wirel. Propag. Lett.*, vol. 10, pp. 1190-1193, 2011.
- [8] M. A. Dorostkar, M. T. Islam, and R. Azim, "Design of a novel super wide band circular-hexagonal fractal antenna," *Prog. Electromagn. Res.*, vol. 139, pp. 229-245, 2013.

- [9] P. Khanna, A. Sharma, A. K. Singh, and A. Kumar, "CPW - fed octagonal ring shaped ultra wide band antenna for wireless applications," *Adv. Electromagn.*, vol. 7, no. 3, pp. 87-92, 2018.
- [10] Z. A. Abdul Hassain, A. R. Azeez, M. M. Ali, and T. A. Elwi, "A modified compact bi-directional UWB tapered slot antenna with double band-notch characteristic," *Adv. Electromagn.*, vol. 8, no. 4, pp. 74-79, 2019.
- [11] A. Joshi and R. Singhal, "Gain enhancement in probe-fed hexagonal ultra wideband antenna using AMC reflector," *J. Electromagn. Waves Appl.*, vol. 33, no. 9, pp. 1185-1196, 2018.
- [12] P. R. Prajapati and S. B. Khant, "Gain enhancement of UWB antenna using partially reflective surface," *Int. J. Microw. Wirel. Technol.*, vol. 10, no. 7, pp. 835-842, 2018.
- [13] Z. Yang, H. Jingjianti and Y. Naichang, "An antipodal Vivaldi antenna with band-notched characteristics for ultra-wideband applications," *AEU - Int. J. Electron. Commun.*, vol. 76, pp. 152-157, 2017.
- [14] D. Sankaranarayanan, D. Venkatakirand, and B. Mukherjee, "A novel compact fractal ring based cylindrical dielectric resonator antenna for ultra wideband application," *Prog. in Electromagn. Res.*, vol. 67, pp. 71-83, 2016.
- [15] A. Kumar, S. Dwari, G. P. Pandey, and B. K. Kanaujia, "A high gain wideband circularly polarized microstrip antenna," *Int. J. Microw. Wirel. Technol.*, vol. 74, pp. 125-130, 2018.
- [16] V. Dinesh and G. Murugesan, "A CPW-fed hexagonal antenna with fractal elements for UWB applications," *Appl. Math. Inf. Sci.*, vol. 13, no. 1, pp. 73-79, 2019.
- [17] CST Microwave Studio, ver. 2013, Computer Simulation Technology, Framingham, MA, 2013.
- [18] M. Guerroui, A. Chaabane, and A. Boualleg, "Super UWB grooved and corrugated antenna for GPR application," *Period. Polytech. Electr. Eng. Comput. Sci.*, vol. 66, no. 1, pp. 31-37, 2022.
- [19] A. Chaabane and M. Guerroui, "Printed UWB rhombus shaped antenna for GPR applications," *Iran. J. Electr. Electron. Eng.*, vol. 17, no. 4, 2021.
- [20] R. Azim, M. T. Islam, and N. Misran, "Design of a planar UWB antenna with new band enhancement technique," *Applied Computational Electromagnetics Society (ACES) Journal*, vol. 26, no. 10, pp. 856-862, 2011.
- [21] R. Azim, R. W. Aldhaheri, M. M. Sheikh, and M. T. Islam, "An effective technique based on off-set fed patch to enhance the bandwidth of microstrip planar antenna," *Microw. Opt. Technol. Lett.*, vol. 58, no. 5, pp. 1221-1226, 2016.
- [22] Md. M. Alam, R. Azim, I. M. Mehedi, and A. I. Khan, "Coplanar waveguide-fed compact planar ultra-wideband antenna with inverted L-shaped and extended U-shaped ground for portable communication devices," *Chin. J. Phys.*, vol. 73, pp. 684-994, 2021.
- [23] R. Azim, M. T. Islam, H. Arshad, Md. M. Alam, N. Sobahi, and A. I. Khan, "CPW-fed super-wideband antenna with modified vertical bow-tie-shaped patch for wireless sensor networks," *IEEE Access*, vol. 9, pp. 5343-5353, 2021.
- [24] R. Azim, M. T. Islam, and N. Misran, "Microstrip line-fed printed planar monopole antenna for UWB applications," *Arab. J. Sci. Eng.*, vol. 38, no. 9, pp. 2415-2422, 2013.
- [25] M. Guerroui, A. Chaabane, and A. Boualleg, "A CPW-fed amended U-shaped monopole UWB antenna for surfaces penetrating applications," *IEEE HORA 3rd Int. Cong. Hum. Comput. Int. Optim. Rob. Appl.*, Ankara, TR, Jun. 2021.
- [26] Y. X. Zhang, Y. C. Jiao, H. Zhang, and Y. Gao, "A simple broadband flat-gain circularly polarized aperture antenna with multiple radiation modes," *Prog. Electromagn. Res. C*, vol. 81, pp. 1-10, 2018.
- [27] T. Chen, J. Zhang, and W. Wang, "A novel cpw-fed planar monopole antenna with broadband circularly polarization," *Prog. Electromagn. Res. M*, vol. 84, pp. 11-20, 2019.
- [28] P. Usha and C. Krishnan, "Epsilon near zero metasurface for ultrawideband antenna gain enhancement and radar cross section reduction," *AEU - Int. J. Electron. Commun.*, vol. 119, 2020.
- [29] J. Chatterjee, A. Mohan, and V. Dixit, "Broadband circularly polarized h-shaped patch antenna using reactive impedance surface," *IEEE Antennas Wirel. Propag. Lett.*, vol. 17, no. 4, pp. 625-628, 2018.
- [30] B. Guenad, A. Chaabane, D. Aissaoui, A. Bouacha, and T. A. Denidni, "Compact cauliflower-shaped antenna for ultra-wideband applications," *Applied Computational Electromagnetics Society (ACES) Journal*, vol. 37, no. 1, 2022, pp. 68-77, 2022.
- [31] A. Chaabane and M. Guerroui, "Circularly polarized UWB antenna with question mark shaped patch for GPR applications," *J. Appl. Res. Technol.*, vol. 20, no. 3, pp. 274-283, 2022.



Djelloul Aissaoui received his Magister degree in signals and systems and his Ph.D. degree in telecommunications science from the University of Tlemcen, Algeria, in 2007 and 2019, respectively. He is currently working as an associate professor in the Department of Electrical Engineering, Faculty of Science and Technology, University of Djelfa, Algeria. His current research areas of interest include fractal antennas, ultra-wideband antennas, and metamaterial antennas.



Abdelhalim Chaabane received his Ph.D. and completed his habilitation in Electronics in 2017 and 2020, respectively. He is currently working as an associate professor and a member of the Telecommunications Laboratory at the University 8 Mai 1945 Guelma. His current research areas of interest include fractal antennas, millimeter-wave high-gain, and wide-band antennas, UWB applications and radar, and biomedical engineering.



Noureddine Boukli-Hacene was born in 1959 in Tlemcen, Algeria. He received his Doctorate Degree (prepared at the “Centre National d’Etudes Spatiales” in Toulouse, France), in Electrical Engineering from the University of Limoges, France, in 1985. Then he joined the University of Tlemcen. Currently, he is a Professor in Electrical Engineering at the same university. His research interests include, among others, microstrip and miniaturized antennas, fractal antennas, ultra-wideband antennas, metamaterial antennas, and microwave circuits.



Tayeb A. Denidni received M.Sc. and Ph.D. degrees in Electrical Engineering from Laval University, Quebec City, QC, Canada, in 1990 and 1994, respectively. From 1994 to 2000, he was a Professor with the Engineering Department, Université du Quebec in Rimouski (UQAR), Rimouski, QC, Canada, where he founded the Telecommunications laboratory. Since August 2000, he has been with the Institut National de la Recherche Scientifique (INRS), Université du Quebec, Montreal, QC, Canada. His current research areas of interest include reconfigurable antennas using EBG and FSS structures, dielectric resonator antennas, metamaterial antennas, adaptive arrays, switched multi-beam antenna arrays, ultra-wideband antennas, microwaves, and development for wireless communications systems.